9C.4 IMPROVING TROPICAL CYCLONE TRACK AND INTENSITY FORECASTING WITH JPSS IMAGER AND SOUNDER DATA

Galina Chirokova*
CIRA/CSU, Fort Collins, CO, USA

Mark DeMaria
NOAA/NWS/NCEP/NHC, Miami, FL, USA

Robert DeMaria and Jack Dostalek
CIRA/CSU, Fort Collins, CO, USA

Jack L. Beven
NOAA/NWS/NCEP/NHC, Miami, FL, USA

Abstract

The Suomi National Polar-Orbiting Partnership satellite (SNPP) launched in October, 2011, is part of the Joint Polar Satellite System (JPSS), the next generation polar-orbiting operational environmental satellite system. SNPP carries five instruments, including Visible Infrared Imaging Radiometer Suite (VIIRS) and Advanced Technology Microwave Sounder (ATMS). The time scale of tropical cyclone track and intensity changes is on the order of 12 hours, which makes JPSS instruments well suited for the forecasting of these parameters. Two basic methods exist for improving tropical cyclone forecasts with SNPP. First is to assimilate data in numerical forecast models, and second is to improve analysis and statistical post-processing forecast products. Our group is developing two applications focusing on the second approach.

The first application, the tropical cyclone Maximum Potential Intensity (MPI) estimate algorithm, is using temperature and moisture retrievals from ATMS in the near storm environment to improve intensity analysis and forecasting. While tropical cyclone track errors have improved dramatically over the past few decades, the ability to forecast intensity changes has improved much more slowly. An especially difficult but very important forecast problem is predicting rapid changes in tropical cyclone intensity. Improving these forecasts is one of the highest priorities within NOAA. Accuracy of both, the Logistic Growth Equation Model (LGEM), the most accurate of the statistical models over the past few years, and the Rapid Intensification Index (RII) tool critically depends on the accuracy of the MPI estimate. Operational versions of LGEM and RII use statistical MPI calculated from Sea Surface Temperature (SST) only. We investigate the use of ATMS-MIRS retrievals as input into the MPI algorithm to improve RII and LGEM forecasts. The MPI algorithm was adapted for use with ATMS temperature and moisture profiles. Preliminary estimates for the Atlantic basin show up to 4.6% Brier Skill Score increase in RII estimates. Newly available data are being incorporated into existing intensity estimation techniques and into LGEM to improve their performance. Results of improved MPI estimates for the Atlantic, as well as the East and West Pacific Basins, will be presented together with a discussion of implications for LGEM forecast performance.

The second application, the multi-spectral center fix algorithm, uses ATMS and VIIRS data for improving center location estimates of tropical cyclones. Estimating the center location is one of the first steps in the forecast process. The accurate center estimate impacts all downstream forecasts, providing better satellite intensity estimates and better numerical model forecasts. Currently, most existing operational center fix methods are subjective, and little investigation has been made into the use of objective techniques. The goal of this project is to improve real-time estimates of tropical cyclone centers using machine learning methods in conjunction with newly available satellite data. Preliminary results from using pressure estimates only from AMSU statistical temperature retrievals for the Atlantic, for the years 2006-2011 (total of 2012 cases), showed 10% improvement in accuracy in comparison to the storm center first guess estimates available in real time. The analysis is being improved by using ATMS data together with multi-spectral imagery from VIIRS, including the low-light imager. Results of the improved analysis will be presented together with the discussion of the possible forecast improvements.

1. INTRODUCTION

Improving tropical cyclone (TC) track and intensity forecasts will lead to improved warnings and longer lead times for mitigation activities from TCs. The Suomi National Polar-Orbiting Partnership satellite (SNPP) launched in October, 2011, is part of the Joint Polar Satellite System (JPSS), the next generation polar-orbiting operational environmental satellite system. SNPP carries five instruments, including Visible Infrared Imaging Radiometer Suite (VIIRS) and

* *Corresponding author address*: Galina Chirokova
CIRA, Colorado State University,
1375 Campus Delivery,
Fort Collins, CO 80523-1375
e-mail: Galina.Chirokova@colostate.edu

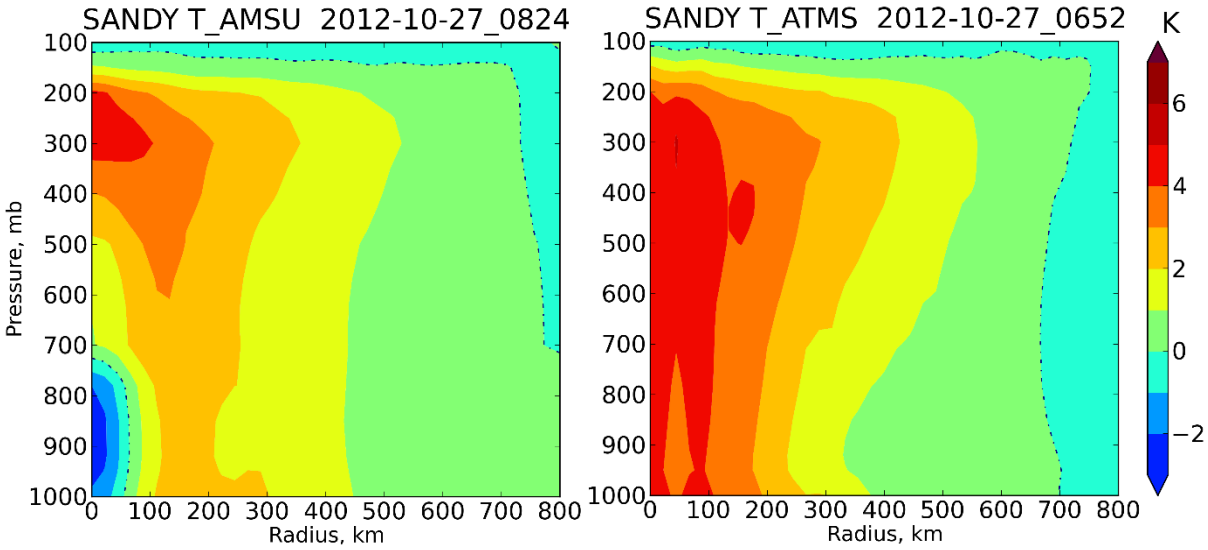

Figure 1. Hurricane Sandy azimuthally averaged temperature profile anomaly, October 27, 2012. The anomaly is calculated relative to the mean vertical profile (weight averaged by radius). AMSU retrievals shows artificial cold bias al low levels, while ATMS better resolves warm core and does not produce artificial cold bias.

Advanced Technology Microwave Sounder (ATMS). The time scale of TC track and intensity changes is on the order of 12 hours, which makes JPSS instruments well suited for the forecasting of these parameters.

Two basic methods exist for improving TC forecasts with SNPP. The first is to assimilate data in numerical forecast models, and the second is to improve analysis and statistical post-processing forecast products. Our group is developing two applications, focusing on the latter approach. The first application uses temperature and moisture retrievals from ATMS in the near storm environment to improve intensity analysis and forecasting. This new information is being incorporated into existing intensity estimation techniques and to operational statistical-dynamical intensity forecast models, including the Logistic Growth Equation Model (LGEM), to improve their performance. The second uses VIIRS and ATMS data for improving center location estimates of TCs, which is the starting point for TC forecasts. Methods are being developed to use multi-spectral imagery from VIIRS, including the low-light imager, in combination with sounder data for this purpose. These new products will be made available in the satellite Proving Ground to operational forecasters at the National Hurricane Center (NHC) and Joint Typhoon Warning Center (JTWC) for evaluation and feedback. If the evaluation is positive, the products can be transitioned to NHC and JTWC operations.

The paper is organized in the following way: 1) in the "data and methods" section we describe ATMS retrievals used for this study, and in the sections 2) and 3) we discuss the results obtained for each of the two applications.

2. DATA AND METHODS

ATMS represents a significant improvement in temperature and moisture retrievals over the current Advanced Microwave Sounding Unit (AMSU) instrument. Finer resolution and wider scan swath width result in better and more frequent TCs observations, along with a larger number of usable soundings. Compared to AMSU, ATMS has almost twice the resolution at nadir (26 km ATMS vs. 52 km AMSU) in some channels, and the ATMS swath width is 2503 km compared to the 2200 km AMSU swath width. The most important improvement for TC applications is that ATMS has temperature and moisture sounding channels combined on the same instrument, including one new temperature channel (51.7 GHz) for sounding the lower troposphere, and two new moisture channels (183 +- 1.8 GHz and 183 +- 4.5 GHz), which were not previously available on AMSU. Further details of ATMS instrument can be found in Weng et al. (2012).

In addition to the new instrument, ATMS data are processed with the new Microwave Integrated Retrieval System (MIRS) retrieval scheme (Boukabara et al., 2011), which offers several advantages over the current statistical retrievals utilized in our previous work. Thus, ATMS-MIRS is better resolving the TC warm core, and the simultaneous retrieval of temperature and moisture profiles allows significant reductions in the artificial cooling in the areas of high cloud liquid water and ice scattering, which are strongly affecting statistical AMSU retrievals (Bessho et al., 2006; Demuth et al., 2004). Figure 1 shows comparison of azimuthally-averaged vertical temperature profile between AMSU and ATMS retrievals, on October 27, 2012. These

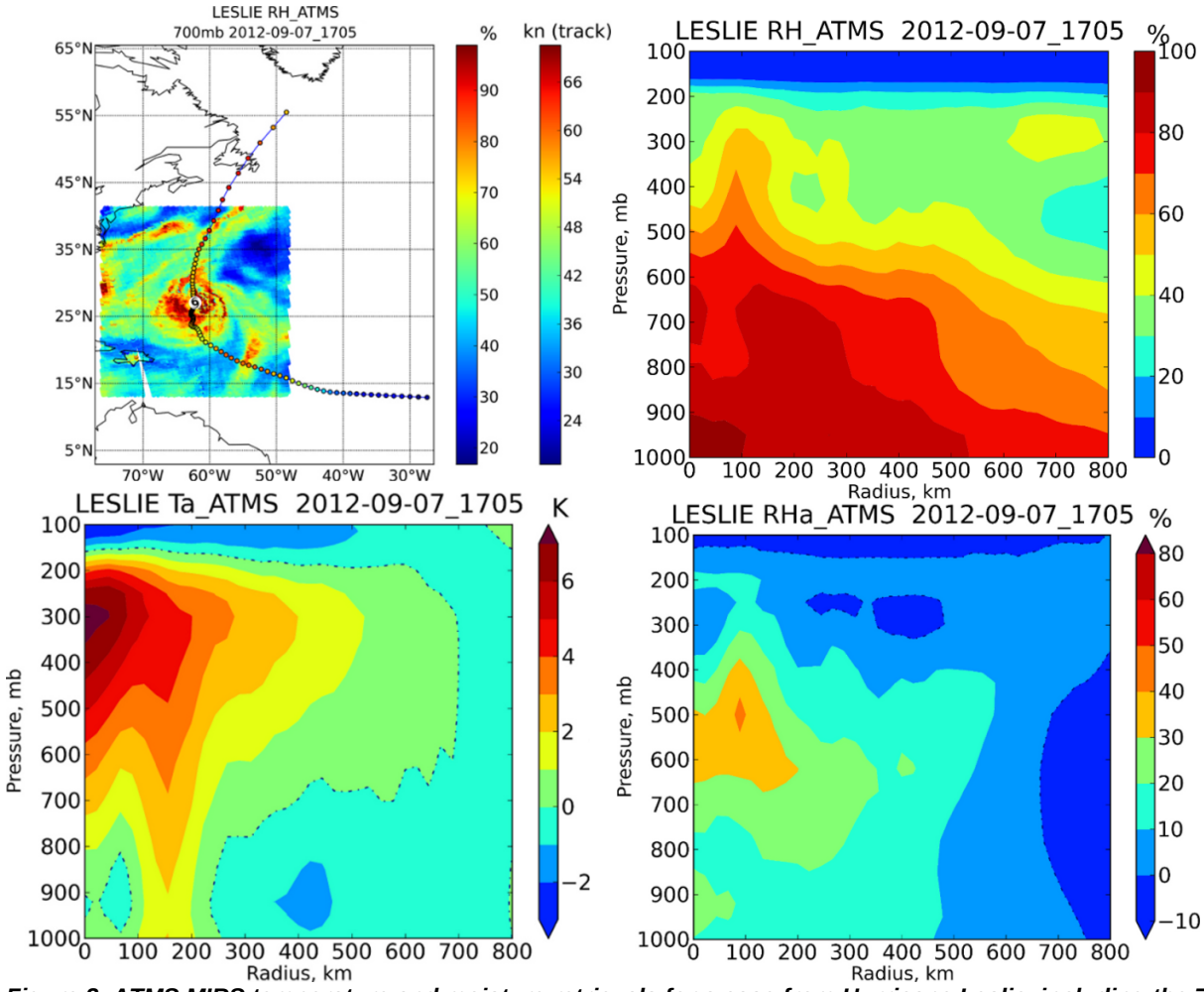

Figure 2. ATMS MIRS temperature and moisture retrievals for a case from Hurricane Leslie, including the 700 hPa relative humidity field (RH) (upper left), and radial-height cross sections of RH (upper right), temperature anomaly (lower left) and RH anomaly (lower right).

profiles are only about one hour apart, and therefore, the differences should be attributed to the differences in retrieval algorithms and instruments. The statistical AMSU retrieval is producing pronounced artificial cold-bias at low levels. ATMS retrievals, for which both temperature and moisture profiles are used, better resolve the warm core, and do not produce this artificial cold bias. Based on this result, we expect to obtain better wind retrievals from ATMS for the center fix algorithm and better representation of the near storm environment for the intensity forecast applications.

The MIRS temperature and moisture retrievals become operational in Feb 2014. A large sample of cases produced using the same algorithm and in the same format as those that became available operationally were obtained from NESDIS/STAR. This sample includes 43 days for 23 TCs from 2012, and 21 days for 15 TCs from 2013, providing over 300 cases from the 2012 and 2013 hurricane and typhoon seasons. This dataset is being used for the majority of the algorithm testing described below.

In the MIRS retrievals the water vapor is retrieved in terms of mixing ratio. We developed methods to convert it to relative humidity (RH), analyze the data in storm-centered coordinates, perform azimuthal averages, and generate perturbation fields. Figure 2 shows an example of a 700 hPa RH field for Hurricane Leslie from the 2012 Atlantic season (upper left). The temperature anomaly plot (lower left) shows a very realistic warm core structure, which does not require low-level correction for high cloud liquid water (CLW) and ice scattering (Demuth et al., 2004). The structure of the moisture fields as seen in the the radial-height cross sections of the azimuthally averaged RH (upper right), and RH anomaly (lower right) look very reasonable, with RH increasing near the storm center. Preliminary comparison shows that

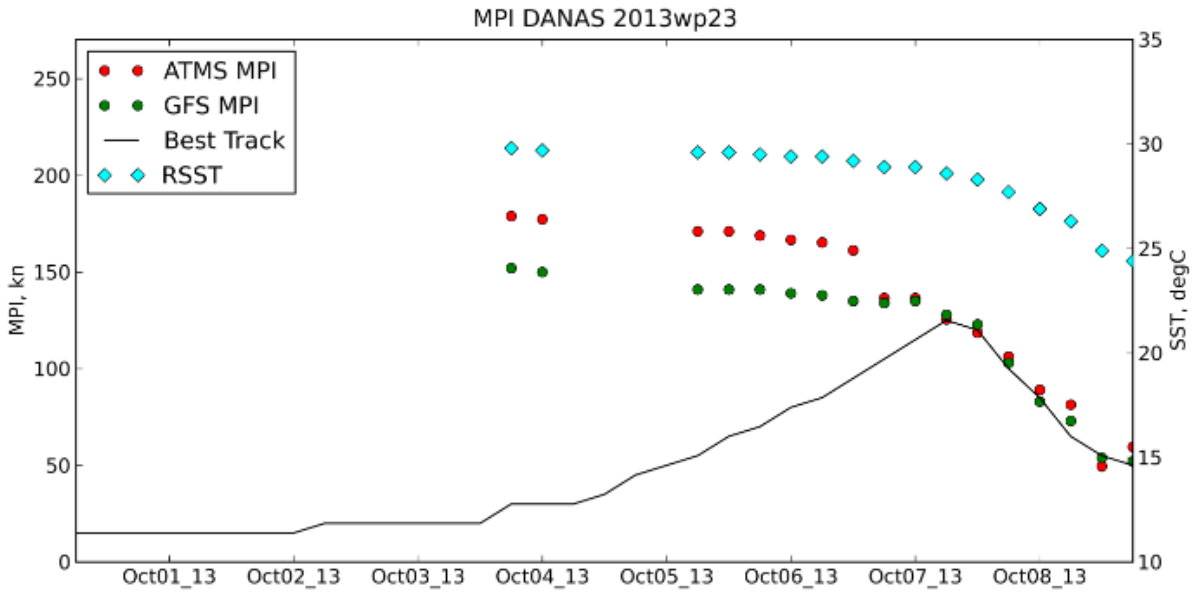

Figure 3: MPI estimate for 2013 Typhoon Danas (WP23) Shown: Best Track intensity (black line), ATMS MPI at swath times (red dots) and GFS MPI at synoptic times (green dots). Weekly Reynolds SST at the storm center (cyan rombs) used for both MPI calculations is shown for reference.

RH values at 600 km from the storm center are similar to Jordan mean tropical sounding (Dunion et. al, 2008), and RH values near the center of the storm are similar to dropsondes data (not shown).

3. MAXIMUM POTENTIAL INTENSITY ESTIMATE

TC track errors have improved dramatically over the past few decades, primarily due to improvements in data assimilation and forecast models. However, the ability to forecast intensity changes has improved much more slowly (DeMaria et al. 2007; DeMaria et al. 2014). An especially difficult but very important forecast problem, especially for storms close to land, is predicting rapid changes in TC intensity. Improving these forecasts is one of the highest priorities within NOAA. Because of the importance of this problem, an operational tool called the Rapid Intensification Index (RII) has been developed (Kaplan et al, 2010). The RII uses a subset of the input to LGEM forecast in a discriminant analysis algorithm to estimate the probability of rapid intensity changes.

3.1 Maximum Potential Intensity estimate from ATMS data

The accuracy of the LGEM forecast, the most accurate of the statistical models over the past few years, critically depends on the accuracy of the Maximum Potential Intensity (MPI) estimate. Currently, the operational LGEM and RII at National Hurricane Center (NHC) use the MPI calculated from a simple statistical algorithm (DeMaria and Kaplan, 1994), which only uses SST data and does not take into account temperature and moisture soundings. We investigate the use of ATMS-MIRS retrievals as input into the more general Bister and Emanuel (1998) MPI algorithm to improve RII forecast. Following Emanuel (1988) and Bister and Emanuel (1998), MPI can be calculated from ATMS-MIRS T,q, and SLP together with SST data as

$$(MPI) = \frac{T_s - T_o}{T_o} \frac{C_k}{C_D} (k^* - k), \qquad (1)$$

where T_s and T_o are the surface temperature and the temperature at the outflow level; k^* and k are the saturation enthalpy of the sea surface and the actual enthalpy of the boundary layer air, respectively; and C_k/C_D is the specified ratio of surface exchange coefficients for momentum and enthalpy. T_s,T_o, k^*, and k are estimated from soundings and SST.

Algorithms were developed to calculate ATMS temperature and RH soundings, and the MPI algorithm was successfully adapted to use as input the ATMS retrievals. Bister and Emanuel (1998) MPI was calculated for all 2012 and 2013 cases in the preliminary MIRS dataset. The MPI algorithm is very sensitive to SST used as input. In order to separate the effect of the SST input from the effect of different atmospheric profiles, as calculated from GFS model and ATMS, all estimates were processed using the same weekly Reynolds SST temperature that was used in the operational version of SHIPS and LGEM. Figure 3 shows a comparison of the MPI estimates from two datasets for Typhoon Danas from 2013 north West Pacific season, the MPI calculated from Bister and Emanuel (1998) theoretical formula with storm

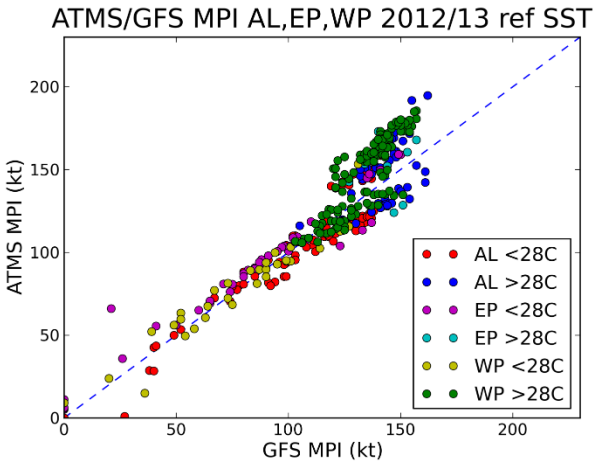

Figure 4: Bister and Emanuel (1998) MPI (kt) calculated from ATMS and GFS moisture and temperature profiles, with all other parameters kept identical. The dots are colored by the SST at the center of the storm above or below 28 ^{o}C, and by basin. The red and blue dots show AL storms with SST at the storm center below and above 28^{o}C, correspondingly; magenta and cyan dots show the same for EP, and yellow and blue dots – for WP. The atmospheric profiles, including temperature and moisture profiles, and sea level pressure (SLP) are calculated from either ATMS or GFS, while all other parameters, including SST, are kept identical. T, q, SLP are averaged between 200 and 800 km for all calculations.

environmental soundings from the GFS analysis (green circles), and the MPI calculated from the same formula with environmental soundings from ATMS (red circles). Also shown in this figure are the weekly Reynolds SST (Reynolds et al., 2007) values that were used to calculate both MPI estimates. There are significant differences between the MPI results, with the ATMS input resulting in higher values during the storm intensification. Figure 4 shows the scatter plot of MPI with GFS versus ATMS sounding input, with the dots colored by the SST at the center of the storm above or below 28^{o}C, and by basin. The T, q profiles and sea level pressure (SLP) for all calculations were averaged between 200 km and 800 km to represent near-storm environment. The weekly Reynolds SST, used in all calculations, is a single point value at the storm center. The ATMS MPI is similar to GFS MPI for weaker storms for AL, EP, and WP storms. For MPI greater than about 100 kt, in some cases the GFS MPI is larger than ATMS MPI, and in some cases that relationship is reversed. The reasons for these differences are being investigated. The differences shown in Fig. 3 indicate that the replacement of the GFS soundings with those from ATMS will have some impact on the LGEM forecasts, since both SHIPS and LGEM use MPI as one of the main parameters. The related RII will also be impacted by this change. The forecast impact on the RII and LGEM is discussed below.

3.2 Effect of using different MPI estimate on the Rapid Intensification Index

The RII estimates the probability that a storm will rapidly intensify, as indicated by a 30 kt or greater increase in the maximum wind in the following 24 h. The newest version of the RII also provides probability estimates for 25, 35 and 40 kt increases in 24 h. The RII has also been adapted to run with the new MPI estimates with ATMS. RII is calculated based on current MPI and four predicted MPI values at 6 h intervals along the forecasted storm track. As the initial value we used the calculated ATMS MPI, and as predicted values we used GFS MPI corrected by the initial difference between the ATMS and GFS MPI values. This work uses preliminary pre-operational ATMS-MIRS dataset, and as result, we have a very small number of cases to work with: 130 cases including 13 RI cases for the Atlantic Basin (AL), 176 cases including 31 RI cases for the north West Pacific Basin (WP), and 38 cases including only one RI case for East Pacific Basin (EP). That number of cases is not sufficient to calculate reliable forecast statistics, so the results presented below are preliminary. Sensitivity tests for RII probability (not shown) show that there is considerable forecast sensitivity to the MPI calculation, with RII probability changing by up to 30%.

Figure 5 shows observed and predicted 25 Kt RII probabilities for major hurricane Michael, AL13, 2012. The green bars indicate times for which RI occurred in next 24 hours. Red and blue stars/triangles show RII predicted based on MPI calculated from GFS fields (red) and from ATMS retrievals (blue). Although both RI estimates are somewhat late in that the highest probabilities were for the period after the RI occurred, the ATMS-based RII goes down much quicker after hurricane intensification ended, thus contributing to lower bias and higher Brier Skill Score (BSS).

The recently developed global version of SHIPS/LGEM/RII code was successfully adopted for use with ATMS input. The global version of the code now allows to run LGEM for WP using MPI calculated from ATMS profiles, in addition to AL and EP. Table 1 shows preliminary statistics for RII with ATMS/GFS input for all AL and WP cases. It could be seen that the Brier Score (BS) in all cases is slightly smaller when using ATMS profiles to calculate MPI, which indicates slight improvement. Brier Skill Score (BSS) and bias, which is always smaller when using ATMS profiles, also indicates slight improvement in the RII forecast for all AL and WP cases. These results look encouraging, however, as shown in the last column in Table 1, only a very small number of cases is used for each calculation. Considerably larger sample sizes are required to obtain reliable statistics. The statistics for the EP cases cannot be calculated at this time because we have only one RI case for EP in our database.

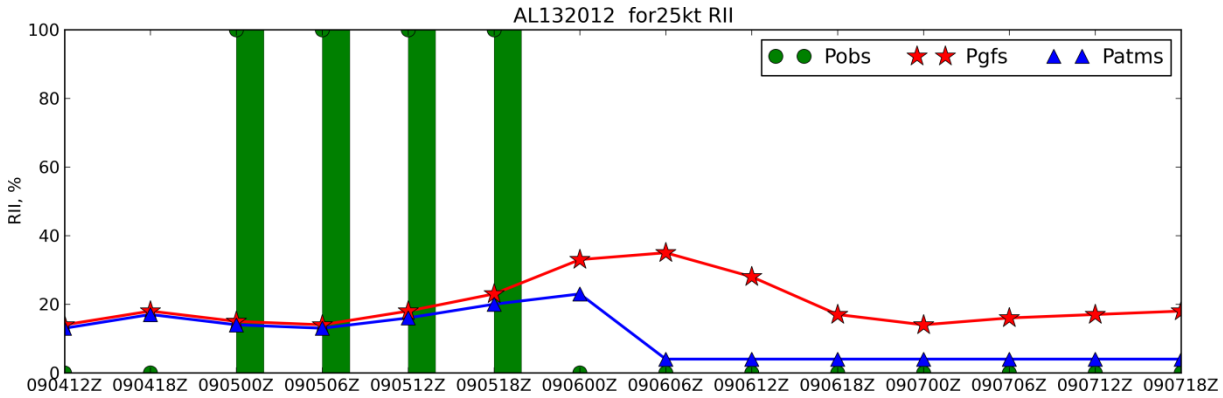

Figure 5: RII for 25 knots for Hurricane Michael, AL13 2013. Green dots show observed RII index, which is 0 if no RI occurred, and 100% if RI occurred. Red line with stars shows RI forecast based on operational GFS model fields, and blue line with triangles shows RI forecast with MPI calculated from ATMS data. The bias of ATMS data is 1.67 compared to 1.87 bias from GFS.

RI	BS GFS	BS ATMS	BS Mean	BSS (%) A/G	BSS (%) G/M	BSS (%) A/M	Bias GFS	Bias ATMS	Basin	# RII Cases
25 kt	964.55	957.98	854.27	0.68	-12.91	-12.14	1.63	1.44	AL	13
30 kt	723.53	718.46	667.83	0.70	-8.34	-7.58	1.30	1.15	AL	10
35 kt	477.11	467.65	413.10	1.98	-15.49	-13.20	1.26	1.00	AL	6
40 kt	248.40	243.55	211.88	1.95	-17.24	-14.95	1.63	1.37	AL	3
30 kt	1044.39	996.30	1586.00	4.60	34.15	37.18	0.56	0.61	WP	31

Table 1: RII statistics for AL (for 25,30,35, and 40 kt) and WP (30kt) basins. The table shows Brier Score (BS), Brier Skill Score in % (BSS), and Bias calculated for RII forecast using MPI calculated from ATMS and GFS profiles. All numbers are based on a very small number of RII cases (last column) and could possibly change as more data becomes available.

3.2 Effect of using different MPI estimate on LGEM intensity forecast

The LGEM model provides a deterministic forecast of maximum wind out to 5 days using a statistical-dynamical approach (DeMaria 2009). The LGEM model was run with MPI calculated from GFS and ATMS profiles, and compared with the operational version. Figure 6 shows LGEM intensity errors comparison between three runs: CTRL run, GFS run, and ATMS run. CTRL is the control run that uses statistical MPI calculated from SST only, and uses the same settings as operational LGEM. GFS run uses GFS MPI, and ATMS run uses MPI estimated from ATMS profiles. Unlike RII, which is a short-term forecast (24 hours), the LGEM intensity forecast is made up to 5 days, and therefore it is less likely to be improved by using ATMS-based MPI at a single time at hour zero. As can be seen from Figure 6, for the AL the GFS run shows slight improvement over control run, however, the ATMS run performs much worse than GFS run and CTRL. For EP both GFS run and ATMS run show slight improvement up to 60 h, and for WP the ATMS runs shows better results than the GFS run, however both are worse than the CTRL run. Again, all these results should be considered preliminary because of the small number of the available cases. We are investigating several possibilities that might contribute to better forecasts for both RI and intensity, including using dropondes to access the quality of ATMS data in the TC environment, and using a combination of GFS and ATMS data to obtain most realistic soundings and surface data to use as input to MPI algorithm.

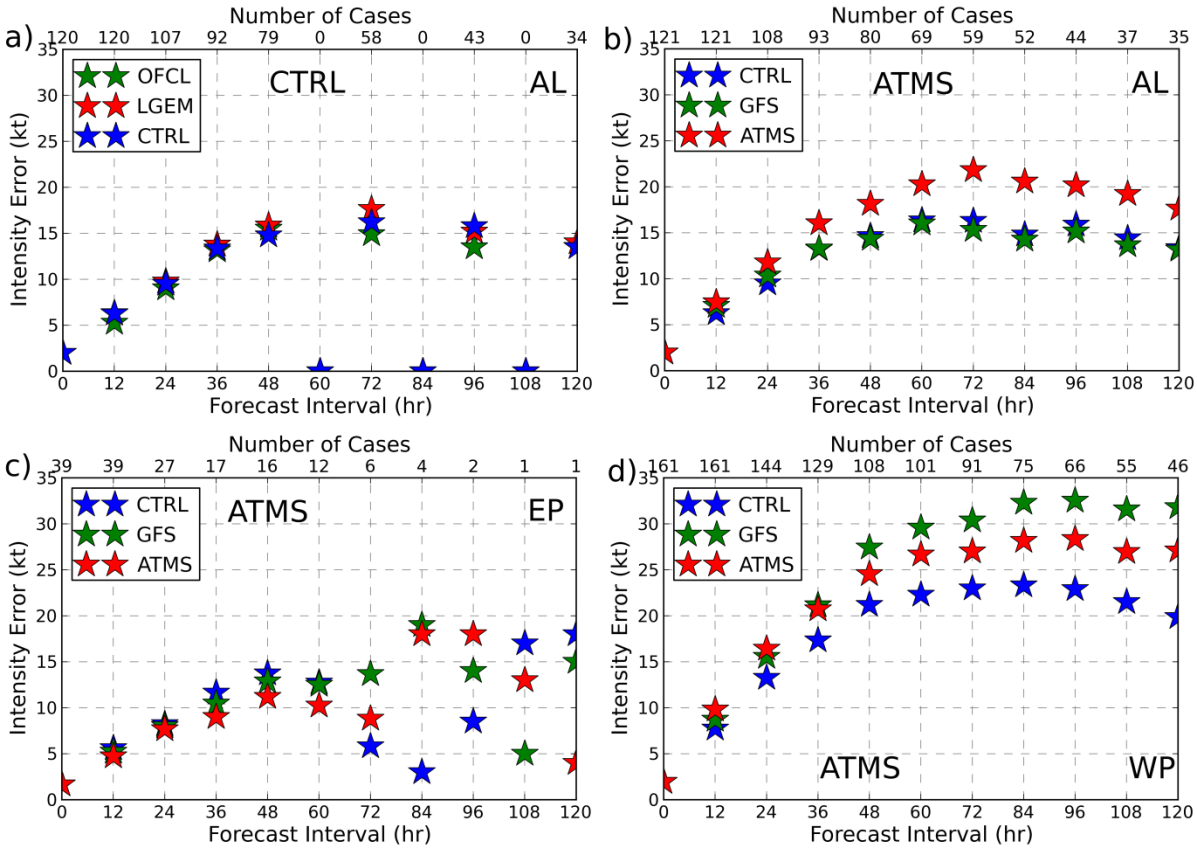

Figure 6. LGEM forecast intensity errors. a) Official NHC forecast (green stars), operational LGEM foracast from NHC (red stars), and operational LGEM rerun at CIRA, (blue stars). b) LGEM forecast for AL basin as run at CIRA using operational LGEM (blue stars), LGEM with MPI calculated from GFS (green stars), and LGEM wuth MPI calculated from ATMS soundings (red stars). c) Same as b), but for EP. d) Same as b), but for WP.

4. CENTER-FIX ALGORITHM

When a TC has formed, typically the first step in producing a forecast is to perform a center-fix to estimate the location of the low-level circulation center of the storm. An accurate center estimate is necessary to prevent initial errors from impacting later steps in forecast production. While aircraft reconnaissance can be used to produce highly accurate center estimates, only about 30% of all TC forecasts have aircraft data available for their production in the Atlantic, and most other TC basins have no aircraft data. Satellite data are available at a much higher rate; however, most of the existing center-fix algorithms are subjective, and due to the limited amount of time that forecasters have to perform prediction for TCs, satellite imagery is an underutilized resource for performing center-fixing. The only existing objective center-fix algorithm developed by Wimmers and Velden (2010) is primarily using spiral patterns in microwave imager data, but does not use microwave sounder data. Our technique uses microwave sounder data, which provides a more physical representation of a cyclone, to estimate pressure, and is novel in its use of techniques from the field of machine learning. Additionally, one of the aims of the proposed method is to improve performance for weak storms.

Because of the fairly coarse resolution of the microwave sounder data relative to IR and visible imager data, both will likely be needed to determine the best estimate of the TC center position. Methods for microwave and IR/vis data are first developed separately, with the goal of combining them in an optimal way. The microwave sounder algorithm is described first, followed by the IR/vis technique. Since a large sample of ATMS data is not yet available, the microwave sounder technique was tested primarily using AMSU data.

4.1 Quadratic Discriminant Analysis of microwave data

Using the hydrostatic integration of temperature retrievals (AMSU for initial testing), the proposed algorithm poses the center-fixing problem as a variation of a classification problem. That is, using a grid-cell in an AMSU retrieval field as input, the output

of the algorithm should be a value indicating the probability that the grid-cell contains a storm center (class A) and a value indicating the probability that the grid-cell does not contain a storm center (class B). Due to its relative ease to implement, Quadratic Discriminant Analysis (QDA) was selected as the algorithm to perform the classification (Bishop, 2006). In order to perform the classification, QDA must be trained. A large dataset of statistical AMSU retrievals, from 2006-2011, was used to train the algorithm. The dataset was assembled by randomly selecting 70% of the available retrievals from 2006-2011 and further selecting only cases that had times that fit between the beginning and end of the appropriate NHC best-track file. Additionally, only retrievals where the storm under examination had maximum winds over 35 kt were included. The retrievals within the remaining 30% of available data that met the same criteria were selected to be the test data set. The training set consisted of 1605 AMSU retrievals and the testing set consisted of 416 AMSU retrievals.

A small dataset of ATMS-MIRS retrievals from 2012 was also made available for use with this algorithm. Using the same method as described above, a training set of 146 ATMS retrievals and a testing set of 90 ATMS retrievals were assembled. Additionally, a testing set using all 236 ATMS retrievals was assembled for use with the AMSU training set.

For each retrieval, a 5x5 grid-cell area around the real-time center fix provided by the NHC forecast from the first synoptic time before the time of the AMSU data (referred to as the extrapolated point) was selected. The grid contains the 700 hPa geopotential height fields determined from the hydrostatic integration of the AMSU or ATMS retrievals. The grid spacing is 0.2 latitude/longitude. The center-location reported by the NHC best-track was then calculated by generating a spline path through the locations in the appropriate best-track file and finding the interpolated position corresponding to the retrieval time. Further, each grid-cell was examined to determine if the best-track center position was located within the grid-cell and marked as the appropriate class. Using this training dataset, QDA was used to generate a function for each of the two classes relating the input values to the probability that they belong to that class. These functions are referred to as discriminant functions. The inputs to the discriminant functions are the geopotential height field and several parameters derived from it, including the distance from the grid point with the height minimum, and the magnitude of the horizontal height gradient. Once these two functions have been generated, center-fixes can then be performed for any retrieved geopotential height field. First, a 5x5 grid-cell area around the extrapolated point is selected. The geopotential height field and derived parameters from these grid-cells are then used as input to both classifier (discriminant) functions. The value for the class B discriminant function is then subtracted from the value returned from the class A discriminant function for each grid-cell. The grid cell with the maximum difference value is selected as the grid-cell that is most likely to contain the storm center for that retrieval.

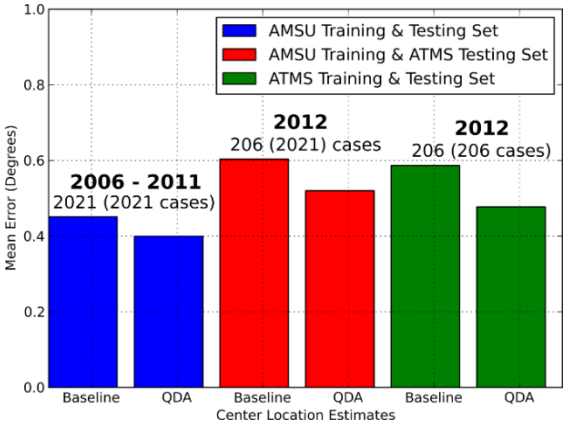

***Figure 7*: Errors in the center location estimate using the NHC best track positions interpolated to the time of the microwave pass. For each pair of bars (blue, red green), the left bar is the error of the first guess position and the second one is the error after the first guess has been updated using the quadratic discriminant analysis (QDA) technique. Results show that using the ATMS data provides a bigger improvement than the AMSU data, even for the case where the algorithm trained on AMSU data is used with ATMS input.**

To evaluate the performance of the center-fix algorithm we compare the distances from the storm center reported by NHC best-track to 1) the storm center estimated by our algorithm and 2) to the extrapolated position (baseline distance). Figure 7 shows the results of three tests which were performed to measure the performance of the center-fix algorithm: the AMSU trained algorithm run against the AMSU test set (AMSU-AMSU, blue bars), the 146 ATMS retrieval trained algorithm run against the 90 ATMS retrieval test set (ATMS-ATMS, red bars), and the AMSU trained algorithm run against the 236 ATMS retrieval test set (AMSU-ATMS, green bars). The real-time center fixes for the AMSU-AMSU test had a mean error of 0.451 degrees, while the output of the center-fix algorithm produced a mean error of 0.400 degrees. The real-time center fixes for the ATMS-ATMS had a mean error of 0.604 degrees compared to the center-fix algorithm mean error of 0.520 degrees. The real-time center fixes for the AMSU-ATMS test had a mean error of 0.587 degrees and the center-fix algorithm had a mean error of 0.477 degrees. So for the AMSU-AMSU, ATMS-ATMS, and AMSU-ATMS tests the center-fix algorithm saw an improvement over the real-time extrapolated center fixes of 11%, 14% and 19% respectively. It should be noted that the ATMS training and testing sets are very small and represent preliminary results. The ATMS

training and testing sets will be expanded in the future as more ATMS data becomes available.

4.1 Circular Hough Transform of infrared data

As described above, the sounder data can provide center estimates to improve upon the extrapolated position. However, the higher resolution VIIRS data will be needed to further refine these estimates. For that purpose, preliminary tests have been performed to investigate the use of a computer vision algorithm on IR data. The algorithm, known as the circular Hough transform (CHT), is a well-known computer vision algorithm for finding circular features in imagery (Swaminathan et al. 2013). A description of the algorithm and its use identifying circular features in ultrasound imagery of nuclear reactors can be found in Swaminathan et al., 2013. An implementation of the algorithm was produced and run on infrared images containing tropical cyclones at various points in their lifetimes. A total of five storms were selected for the initial examination. Each storm was selected to be representative of a type of TC that may be encountered by a center-fixing routine. The following list provides the name of each storm and the type of storm it represents:

- Charley 2004 – Very small but intense hurricane
- Katrina 2005 – Classic large, intense hurricane
- Erika 2009 – Very disorganized weak tropical cyclone, did not make it to hurricane strength
- Earl 2010 – Strong hurricane in higher latitudes
- Sandy 2012 – Unusually large but only moderate strength, non-classical hurricane structure

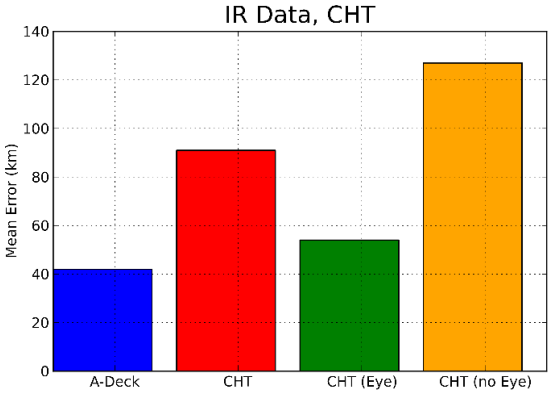

Figure 8: Mean errors reported from using the circular Hough transform on IR images to perform automatic center fixing. Shown are: A-Desk errors (blue bar), CHT errors for all cases (red bar), CHT errors for images containing an eye (green bar), and CHT errors for images without an eye (yellow bar).

The entire lifetime of each of these storms at 6 h intervals was examined, thus making a total of 135 IR images used to evaluate the CHT performance. GOES data were utilized since the VIIRS data was not available for most of these cases. The distance between the center location reported by the algorithm and the best-track location was computed for each image. Additionally, the distance between the real-time location produced by the NHC, extrapolated to the time the IR image was created, and the best-track was used as a baseline comparison. The results can be seen in Figure 8. While the algorithm performed fairly well on images containing an eye, greater error was experienced when no eye was present. However in cases without an eye, the algorithm was able to effectively find the center of the cloud shield. Relating the center of the cloud shield to the rotational center of the storm may be an effective method of performing automated center-fixing and further work will be performed to investigate this possibility. For the weaker systems, additional information will be needed such as spiral cloud lines from visible and day-night band imagery, circulation centers and vertical wind shear estimates from ATMS wind retrievals.

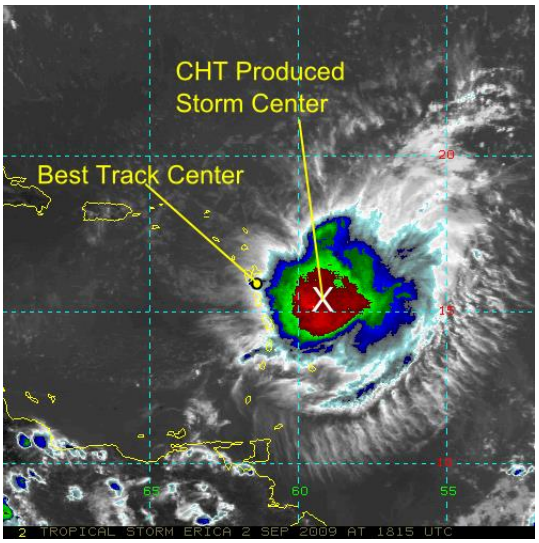

Figure 9. The IR image of TC Erika (AL06, 2009) illustrates the case where the rotational center of the storm is located outside of any circular structure in the image and thus the CHT algorithm is unable to generate a center estimate near the true center.

The difference in performance between images with and without an eye has a fairly straightforward explanation. The algorithm was able to successfully identify the center of circular features in the imagery such as the center of eyes as well as the center of cloud shields. Unfortunately, in many cases, vertical wind shear shifts the rotational center of the storm far from the center of its cloud shield. A particularly extreme case can be seen in Figure 9.

In this image of 2009 AL TC Erika, it can be seen that the rotational center was not located within the cloud shield at all, thus causing the center identified by the CHT to be distant from the true center location. In the future, a refinement of the algorithm may be able to use information about the vertical wind shear to produce an improved center fix. One interesting side effect of performing this investigation is that the techniques required to perform the CHT on imagery as well as the CHT itself may lead to the development of a novel technique for performing automatic eye detection from IR imagery. Future work may involve testing related algorithms for performing automatic eye detection.

5. CONCLUSIONS AND FUTURE PLANS

Both LGEM deterministic and RII probabilistic intensity forecasts are critically dependent on MPI estimate, and it has been shown that they both could be significantly altered by using MPI calculated from ATMS profiles. Preliminary results for the RII forecast show slightly improved RII statistics, as estimated by BS, BSS, and bias for both AL and WP with the use of ATMS data, and possibly slight improvement in LGEM intensity forecast for EP for up to 60 hours. Both of these results are very encouraging, and will be further refined as more ATMS-MIRS data become available. In addition we are investigating several possibilities that might contribute to better forecasts of both RII and LGEM, including using dropsondes to access the quality of ATMS data in TC environment, and using combination of GFS and ATMS data to obtain most realistic soundings and surface data to use as input to MPI algorithm.

Center fixing using QDA with microwave sounder retrievals as input showed up to 19% better center location as compared to the first guess position from the NHC real-time forecast positions. Although the use of the circular Hough transform did not meet our goals of improving the center-fix, future refinements of the algorithm may produce better results. Additionally, the CHT may prove useful to help solve other related problems such as automatic eye detection. The next step in the center-fix algorithm is the addition of VIIRS data, especially the Day Night Band (DNB) data, to refine the estimates from the microwave sounder input. Finally, both the intensity and the center-fix algorithms could be further improved by using Cross-Track Infrared Sounder (CrIS) data.

DISCLAIMER

The views, opinions, and findings contained in this article are those of the authors and should not be construed as an official National Oceanic and Atmospheric Administration (NOAA) or U.S. Government position, policy, or decision.

REFERENCES

Bishop C.M., 2006: Pattern Recognition and Machine Learning, New York, NY, Springer Science+Business Media, LLC, 749pp.

Bister, M., and K. A. Emanuel, 1998: Dissipative heating and hurricane intensity. *Meteor. Atmos. Phys*., **65**, 233–240. doi:10.1007/BF01030791

Boukabara, S.-A., K. Garrett, W. Chen, F. Iturbide-Sanchez, C. Grassotti, C. Kongoli, R. Chen, Q. Liu, B. Yan, F. Weng, R. Ferraro, T. Kleespies, and H. Meng, 2011: MiRS: An All-Weather 1DVAR Satellite Data Assimilation & Retrieval System. *IEEE Trans. Geosci. Remote Sens*., **49**, no. 9, pp. 3249-3272, Sep. 2011. doi: 10.1109/TGRS.2011.2158438

DeMaria, M., 2009: A Simplified Dynamical System for Tropical Cyclone Intensity Prediction. *Mon. Wea. Rev*., **137**, 68–82. doi: http://dx.doi.org/10.1175/2008MWR2513.1

DeMaria, M., J. Kaplan, 1994: Sea Surface Temperature and the Maximum Intensity of Atlantic Tropical Cyclones. *J. Climate*, **7**, 1324–1334.doi: http://dx.doi.org/10.1175/1520-0442(1994)007<1324:SSTATM>2.0.CO;2

DeMaria, M., J.A. Knaff, and C.R. Sampson, 2007: Evaluation of Long-Term Trends in Operational Tropical Cyclone Intensity Forecasts. *Meteor. and Atmos. Physics*, **97**, 19-28.

DeMaria, M., C. R. Sampson, J. A. Knaff, K. D. Musgrave, 2014: Is Tropical Cyclone Intensity Guidance Improving?. *Bull. Amer. Meteor. Soc*., **95**, 387–398. doi: http://dx.doi.org/10.1175/BAMS-D-12-00240.1

Demuth, Julie L., Mark DeMaria, John A. Knaff, 2006: Improvement of Advanced Microwave Sounding Unit Tropical Cyclone Intensity and Size Estimation Algorithms. *J. Appl. Meteor. Climatol*., 45, 1573–1581. doi: http://dx.doi.org/10.1175/JAM2429.1

Demuth, J. L., DeMaria, M., Knaff, J. A., Vonder Haar, T. H., 2004: Evaluation of Advanced Microwave Sounding Unit Tropical-Cyclone Intensity and Size Estimation Algorithms. *J. Appl. Meteor*., **43**, 282–296.doi: http://dx.doi.org/10.1175/1520-0450(2004)043<0282:EOAMSU>2.0.CO;2

Dunion, J. P. and C. S. Marron, 2008: A Reexamination of the Jordan Mean Tropical Sounding Based on Awareness of the Saharan Air Layer: Results from 2002. *J. Climate*, **21**, 5242–5253.doi: http://dx.doi.org/10.1175/2008JCLI1868.1

Emanuel, K. A., 1988: The Maximum Intensity of Hurricanes. *J. Atmos. Sci.*, **45**, 1143–1155.doi:http://dx.doi.org/10.1175/1520-0469(1988)045<1143:TMIOH>2.0.CO;2

Kaplan, J., M. DeMaria, and J.A. Knaff, 2010: A revised tropical cyclone rapid intensification index for the Atlantic and east Pacific basins. *Wea. Forecasting*, **25**, 220-241.

Reynolds, R. W., T. M. Smith, C. Liu, D. B. Chelton, K. S. Casey, and M. G. Schlax, 2007: Daily high-resolution blended analyses for sea surface temperature. *J. Climate*, **20**, 5473-5496.

Swaminathan, K. and Swaminathan P, 2013: Hough Transform Method for Determining the Fuel Sub-Assembly's In-Situ 'Bow' in Breeder Reactor Using Its Sparsely Scanned Ultrasonic Image. *IEEE Transactions on Nuclear Science*, **60**, no. 4, pt. 2, 3033 - 3039

Weng, F., Zou, X., Wang, X., Yang, S., & Goldberg, M. D. 2012: Introduction to Suomi NPP ATMS for NWP and tropical cyclone applications. *J. Geophys. Res*, **117**, D19112,14PP. doi:1029/2012JD018144

Wimmers, A. J., C. S. Velden, 2010: Objectively Determining the Rotational Center of Tropical Cyclones in Passive Microwave Satellite Imagery. *J. Appl. Meteor. Climatol*., **49**, 2013–2034.doi: http://dx.doi.org/10.1175/2010JAMC2490.1